Original Article

Downregulation of homeobox B8 in attenuating non-small cell lung cancer cell migration and invasion though the epithelial-mesenchymal transition pathway

Suxin Jiang[1,2]^, Tao Wang[1], Yong Han[1], Toyoaki Hida[3], Muhammad Zubair Afzal[4], Chuanhong Zhou[1], Jingna Zhu[1], Huaiyu Wang[1]

[1]Department of Thoracic Surgery, Air Force Medical Center, People's Liberation Army of China, Beijing, China; [2]Graduate School of China Medical University, Shenyang, China; [3]Lung Cancer Center, Central Japan International Medical Center, Minokamo, Gifu, Japan; [4]Hematology-Oncology, Dartmouth Cancer Center, Lebanon, NH, USA

Contributions: (I) Conception and design: H Wang; (II) Administrative support: H Wang; (III) Provision of study materials or patients: S Jiang; (IV) Collection and assembly of data: T Wang; (V) Data analysis and interpretation: C Zhou; (VI) Manuscript writing: All authors; (VII) Final approval of manuscript: All authors.

Correspondence to: Huaiyu Wang, MD. Department of Thoracic Surgery, Air Force Medical Center, People's Liberation Army of China, No. 30 Fucheng Street, Beijing 100142, China. Email: alexpepsi@126.com.

Background: Homeobox (*HOX*) family genes have been identified as regulators of cancer development. No research exists concerning the mechanisms underlying homeobox B8 (*HOXB8*) activity in non-small cell lung cancer (NSCLC). In this study, we investigated expression and biological function in NSCLC to determine whether it is an important marker of patient prognosis.

Methods: *HOXB8* expression in NSCLC tissues was investigated using immunohistochemistry (IHC) and Western blot assays. In addition, *HOXB8* was knocked down in NSCLC cells to assess its biological functions in this context. The invasive and migratory potential of cells was evaluated by using Transwell (BD, Franklin Lakes, NJ, USA) inserts with 8-μm pores. Furthermore, Western blotting was used to explore whether *HOXB8* can influence epithelial-mesenchymal transition (EMT).

Results: *HOXB8* was expressed at high levels in NSCLC tissues and cell lines compared with adjacent normal tissues. Patients with high *HOXB8* expression had shorter survival time and worse prognosis. *HOXB8* expression was associated with pathological grading, tumor size, and lymph node metastasis. HOXB8 was prognostic in patients with NSCLC. After knockdown of *HOXB8* via small interfering RNA, the proliferation, migration and invasion ability of the cells were significantly reduced compared with the control group. Moreover, EMT was inhibited by the downregulation of *HOXB8* expression, as the expressions of E-cadherin was upregulated and that of the N-cadherin, vimentin, matrix metalloproteinase 2 (*MMP2*), and twist were downregulated. *HOXB8* is a member of the ANTP homeobox family and encodes a nuclear protein with a homeobox DNA-binding domain. It is included in a cluster of homeobox B genes located on chromosome 17. The encoded protein functions as a sequence-specific transcription factor that is involved in development.

Conclusions: *HOXB8* is highly expressed in NSCLC and may predict prognosis of patients with this type of cancer. Furthermore, *HOXB8* may promote NSCLC progression through the regulation of the EMT process.

Keywords: Homeobox B8 (*HOXB8*); non-small cell lung cancer (NSCLC); migration

^ ORCID: 0000-0003-1927-4688.

Submitted Dec 21, 2023. Accepted for publication Jan 22, 2024. Published online Jan 29, 2024.
doi: 10.21037/tcr-23-2344
View this article at: https://dx.doi.org/10.21037/tcr-23-2344

Introduction

Lung cancer is one of the most common malignant tumors. According to data released by the National Cancer Center in 2015, the 5-year prevalence rate of lung cancer in China from 2006 to 2011 was 130.2 (1/100,000), among whom 84.6 (1/100,000) were males and 45.6 (1/100,000) were females, ranking second and fourth in malignant tumors in each sex, respectively (1). In 2015, the International Association for the Study of Lung Cancer formulated the eighth edition of the tumor node metastasis staging system for lung cancer. According to the Survey, Epidemiology, and End Results database in the United States, 57% of patients with lung cancer have distant metastasis at initial diagnosis (2); therefore, majority of the lung cancer patients undergoing treatment are the metastatic lung cancer patient. Molecular genetic research into lung cancer has made remarkable progress in recent years (3,4). Molecular typing based on genetic characteristics has led the treatment of advanced lung cancer into the era of individualized molecular targeted therapies (2).

Highlight box

Key findings

- Homeobox B8 (*HOXB8*) was significantly upregulated in non-small cell lung cancer (NSCLC) tissue compared with adjacent normal tissue. Knockdown of *HOXB8* expression could inhibit epithelial-mesenchymal transition (EMT), thereby attenuating the proliferation, migration, and invasion ability of NSCLC cells.

What is known and what is new?

- *HOXB8* promotes the proliferation, migration, and invasion of lung cancer cells by affecting the process of EMT in lung cancer. EMT was inhibited by the downregulation of HOXB8 expression, as E-cadherin expression was upregulated while that of the other proteins was downregulated.
- Patients with high *HOXB8* expression had shorter survival time and worse prognosis. *HOXB8* levels were associated with prognosis in patients with NSCLC.

What is the implication, and what should change now?

- We found that *HOXB8* levels were increased in lung cancer tissues and cells, and that its levels were associated with advanced disease stage and metastasis. *HOXB8* may be an important marker of patient prognosis.

Homeobox genes were first identified in a study of the embryonic development of Drosophila melanogaster (5). Mutations in these genes can lead to ectopic organ growth in eukaryotes. Mammalian homeobox genes can be divided into two categories. Class I *HOX* genes are arranged in series on different chromosomes and contain a conserved 180–183 nucleotide sequence encoding a homologous domain composed of 60–61 amino acids that recognizes DNA sequences with a core 5'-TAT-3' motif and regulates the transcription activity of downstream genes. Class II *HOX* genes are referred to as non-*HOX* or para-*HOX* genes, and include the *PAS*, *DLS*, *Hes*, and *MSX* gene families, among others, which have a wide variety of molecular structures, and are not tandemly distributed on chromosomes (6). There are 39 human *HOX* genes that, according to sequence similarity and chromosome position, can be divided into four clusters: *HOXA*, *HOXB*, *HOXC*, and *HOXD*. Each cluster comprises 1–13 gene loci (including 9–11 genes) and is arranged along a DNA sequence from 3'→5', referred to as *HOX* loci, as follows: *HOXA*, 7p15.3; *HOXB*, 17p21.3; *HOXC*, 12q13.3; and *HOXD*, 2q31. *HOX* genes are closely associated with the control of physiological processes (6,7), acting as major drivers of vertebrate embryonic development; however, the specific roles of *HOX* genes in adult cell differentiation are less clear. Nevertheless, a growing amount of evidence supports the key role for *HOX* genes in the occurrence and development of tumors (8,9).

In this study, we explored the expression of *HOXB8* in lung cancer and its effect on the biological functions of lung cancer cells, including proliferation and migration, and conducted a preliminarily exploration of the mechanism underlying its effects. We present this article in accordance with the REMARK reporting checklist (available at https://tcr.amegroups.com/article/view/10.21037/tcr-23-2344/rc).

Methods

Tissue microarrays

A lung cancer tissue microarray (#HLug-Squ150Sur-02), comprising samples and data from 75 patients with lung cancer, was purchased from Shanghai Outdo Biotech Co.

Ltd. (Shanghai, China). All patients had undergone surgery from 2004 to 2007.

Cell culture and transfections

A549 cells are epithelial cells that grow as an adherent monolayer *in vitro* and serve as suitable transfection hosts. It has become the gold standard for lung cancer research models and are now commonly used in cell culture research as a model for studying human lung cancer. The human lung cancer cell line, A549, was cultured in Dulbecco's Modified Eagle Medium (DMEM) supplemented with 10% fetal bovine serum (FBS) at 37 ℃ with 5% CO_2. *HOXB8*-targeting small interfering RNAs (siRNAs) were ordered from Jima Company (Suzhou, China) and transfected into lung cancer cells using Lipofectamine 3000, following the manufacturer's instructions. Cells were cultured in 12-well plates and transfected with 2 μL of siRNA and 3 μg of vectors.

The siRNA sequences were as follows: siRNA1, 5'-GCT CTTATTTCGTCAACTCACTGTTCTCC-3'; siRNA2, 5'-GAGCTGGAGAAGGAGTTCCTATTTAATCC-3'.

Western blotting

Equal amounts of proteins extracted from cells (40 μg per lane) were added to 5× protein buffer, heated at 95 ℃ for 10 minutes (min), then separated with sodium dodecyl sulfate-polyacrylamide gel electrophoresis (SDS-PAGE) until the bromophenol blue in the loading dye reached the bottom of the glass plate. The separated proteins were then electrotransferred to nitrocellulose membranes. Membranes were blocked with 3% skim milk in tris-buffered saline with + 0.5% Tween20 (TBST) at room temperature for 1 hour on a shaking table and subsequently mixed with the antibodies against *HOXB8*, E-cadherin, N-cadherin, vimentin, matrix metalloproteinase 2 (MMP2), twist (all in a 1:1,000 dilution), or anti-β-actin antibody (1:1,500 dilution) and incubated overnight at 4 ℃ via shaking on ice. Antibodies were purchased from Cell Signaling Technology (CST; Danvers, MA, USA). Membranes were then washed 3–5 times for 10 min in TBS and Western buffer, after which horseradish peroxidase (HRP)-labeled secondary antibody was added, with the mixture being incubated at room temperature for 1 h with shaking. Next, membranes were washed with TBST and Western buffer 3–5 times for 10 min each time. Nitrocellulose membranes were dried with filter paper and incubated for 5 min with Enhanced chemiluminescence (ECL) solution (1:1 ratio). Hybridized membranes were analyzed using an ImageQuant gel imaging system (GE Healthcare, Chicago, IL, USA), and the generated images were analyzed using ImageQuant software. GAPDH levels were used as an internal normalization parameter.

Cell proliferation assay

Transfected cells were plated in 96-well plates (1,000 cells/well) and incubated with 10 μL of Cell Counting Kit 8 (CCK-8) solution (BD, Franklin Lakes, NJ, USA) at 37 ℃ for 2 hours, and then the absorption was measured at 450 nm. Proliferation rates were detected at days 1, 2, 3, 4, and 5 after transfection. Proliferation rates were calculated using GraphPad Prism 6.0 software (GraphPad Software, San Diego, CA, USA).

Cell migration and invasion assays

The invasive and migratory potential of cells was evaluated using Transwell inserts (BD, Franklin Lakes, NJ, USA) with 8-μm pores. Matrigel glue was melted with serum-free medium at different proportions (see "Results" section for details), mixed, evenly spread on to the bottom of upper Transwell chambers, and then placed in a 37 ℃ incubator for 2–4 hours until it became gel-like. Chambers were then inoculated with cells in logarithmic growth phase, which were first released by digestion with trypsin, counted, and diluted in serum-free medium. After cells were seeded into the bottom, Transwell chambers were placed in porous plates containing medium supplemented with 10% FBS for culture. Cells were stained and then cultured for 48 hours, the Transwell chambers were then removed, and the cells and residual Matrigel were cleaned off with a cotton swab and washed with phosphate-buffered saline (PBS) 3 times. The cells that had passed through the porous membrane to the bottom were fixed with polymethyl aldehyde, stained with crystal violet, and subjected to microscopic counting and analysis.

Immunohistochemical (IHC) analysis

According to standard protocols, the lung cancer tissues were dewaxed, and antigen retrieval conducted. Tissue sections were dewaxed, washed once with distilled water, repaired with ethylenediaminetetraacetic acid (EDTA) (Beytime, Shanghai, China) (pH 8.0) for 2 min, washed

with PBS for 3 min ×3 times, incubated with 3% H_2O_2 at room temperature for 10 min, washed with PBS for 3 min ×3 times, incubated with animal nonimmune serum at room temperature for 15 min, dried, mixed with 5 μL of anti-I (*HOXB8*) added, and incubated at 4 ℃ overnight. Subsequently, slides were washed with PBS (3 min ×3 times), mixed with 50 μL of secondary antibody working solution, and incubated at room temperature for 15 min. This was followed by further washes with PBS (3 min ×3 times) and a mixture with HRP color reagent and 3-amino-9-ethylcarbozole (AEC) color development, with subsequent color development being observed under microscopy. Once the color developed, slides were washed with distilled water for 5 min, mixed with 2 drops of dye enhancer, washed in PBS (3 min ×3 times), and mixed with 50 μL of cytokeratin (CK) AE1/AE3 (ThermoFisher, Suzhu, China) for overnight incubation at 4 ℃. Slides were then rinsed with PBS (3 min ×3 times), mixed with 50 μL of secondary antibody [alkaline phosphatase-labeled sheep anti-mouse immunoglobin G (IgG) polyclonal antibody] working solution, and incubated at room temperature for 15 min. Samples were then rinsed with PBS (3 min ×3 times). BCIP/NBT (Beytime, Shanghai, China) was used as the color detection reagent for alkaline phosphatase, and the color effect was observed under microscopy. Samples were stained with hematoxylin (Beytime, Shanghai, China) for 10 seconds, washed back to blue with tap water, sealed with AEC water-based sealer, and then sealed with neutral gum. The extent and intensity of HOXB8 staining was evaluated by a pathologist, independently and without access to clinical data.

Using the DM2500 image analysis system (Leica, Wetzlar, Germany), 5 high power fields (400×) were observed and 100 cells counted per field. Samples were scored as follows: no staining =0, light yellow =1, brown-yellow =2, and brown =3; percentage of stained cells ≤5% =0, 6–25% =1, 26–50% =2, and ≥51% =3. Final scores were obtained by multiplying the staining degree of each section by the mean percentage cell staining score according the following schema: <1, negative (–); 2–3 (+), weak positive; 4–6 (++), strong positive; and >6 points (+++), very strong positive (10).

Statistical analysis

The Student's *t*-test (2-tailed) was used for data analysis. Values of P<0.05 were considered significant. Prognosis was analyzed with the Kaplan-Meier method and Cox proportional analysis.

Results

IHC analysis demonstrated that HOXB8 expression was upregulated in NSCLC tissues samples

HOXB8 expression in an NSCLC tissue array was analyzed via IHC analysis. The results showed that the *HOXB8* was expressed at significantly higher levels in cancer tissue than in adjacent normal tissue (shown in *Figure 1*). Furthermore, *HOXB8* was expressed at higher levels in NSCLC tissues with poorer differentiation.

HOXB8 expression was prognostic in NSCLC

We further correlated the IHC *HOXB8* expression level with clinical data. The results showed that *HOXB8* expression was associated with pathological grading, tumor size, and lymph node metastasis with P<0.05 (*Table 1*). We also analyzed the relationship between *HOXB8* expression and patient prognosis and survival. The results showed that patients with high *HOXB8* expression had shorter survival time and worse prognosis (*Table 2* and *Figure 2*).

Knockdown of HOXB8 expression attenuated the proliferation, migration, and invasion ability of NSCLC cells

Since *HOXB8* expression was significantly upregulated in lung cancer cells, we next investigated whether *HOXB8* could affect the biological functions of lung cancer cells. To further discern the role of *HOXB8* in lung cancer progression, we knocked down *HOXB8* expression using siRNAs in two lung cancer cell lines and conducted functional analysis of lung cancer cell cells transfected with *HOXB8* mimics compared with negative controls. A CCK-8 cell proliferation assay demonstrated that the cell proliferation rate in the *HOXB8* siRNA-treated group was lower than that in the negative controls, particularly on day 3 after transfection (*Figure 3*). Furthermore, in Transwell assays, the *HOXB8* siRNA group had fewer cells in the migration chamber relative to controls, while in the Matrigel assay, the *HOXB8* siRNA group also showed fewer cells in the migration chamber, suggesting that *HOXB8* can promote lung cancer cell migration and invasion ability (shown in *Figure 3*).

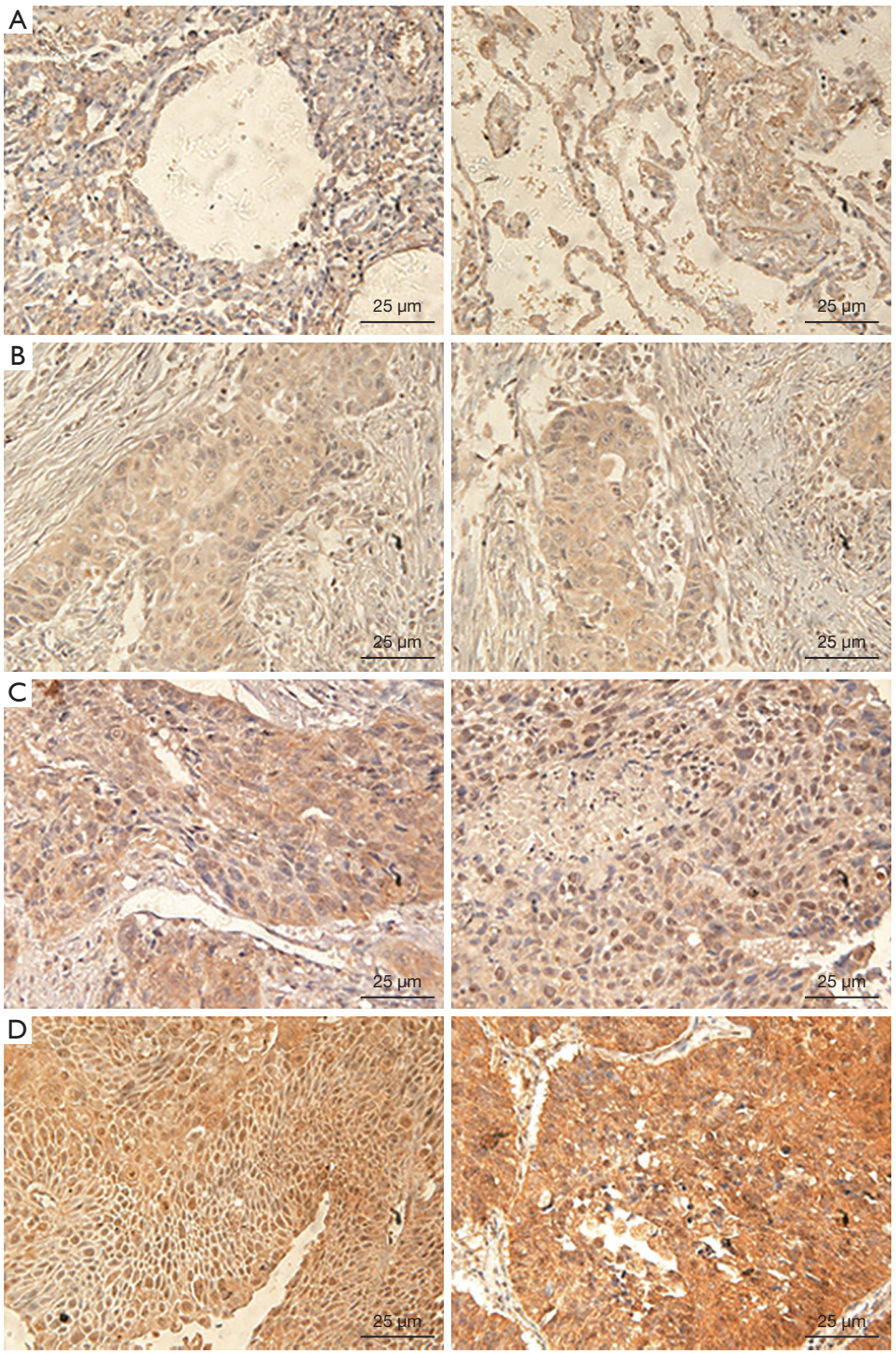

Figure 1 Expression of *HOXB8* immunohistochemistry in different tissues. (A) Adjacent benign tissue; (B) highly differentiated lung cancer tissue; (C) moderately differentiated lung cancer tissue; (D) poorly differentiated lung cancer tissue. Method: immunohistochemistry. HOXB8, homeobox B8.

Table 1 Clinicopathologic variables and the evaluation of *HOXB8* immunostaining in NSCLC tissues

Characteristics	Number of patients					P value
	Total	(–)	(+)	(++)	(+++)	
Age (years)						0.553
>60	52	1	18	16	17	
≤60	33	1	11	11	10	
Sex						0.883
Male	69	2	26	25	16	
Female	6	0	3	2	1	
Clinical stage						0.775
Early stage	52	2	19	19	12	
Advanced stage	23	0	10	8	5	
Histological grade						0.043
High grade	55	2	23	22	8	
Low grade	20	0	6	5	9	
Tumor size (cm)						0.007
>3	62	0	27	22	13	
≤3	13	2	2	5	4	
Lymph node metastasis						0.039
Yes	31	0	8	12	11	
No	44	2	21	15	6	

(–), <1 point (negative); (+) 2–3 points (weak positive); (++) 4–6 points (strong positive); (+++) >6 points (very strong positive). HOXB8, homeobox B8; NSCLC, non-small cell lung cancer.

Table 2 Cox proportional hazards model analysis of prognostic factors in patients with NSCLC

Characteristic	HR	95% CI	P value
Age (≤60/>60 years)	1.999	0.268–14.898	0.499
Gender (male/female)	1.753	0.707–4.347	0.226
Clinical stage (early stage/advanced stage)	1.290	0.766–2.172	0.338
Tumor size (>3/≤3 cm)	0.565	0.186–1.710	0.312
Histologic grade (high grade/low grade)	0.803	0.294–2.193	0.669
HOXB8 staining (weak/strong)	3.514	1.846–6.690	<0.001
Recurrence (yes/no)	1.471	0.624–3.465	0.377

NSCLC, non-small cell lung cancer; HR, hazard ratio; CI, confidence interval; HOXB8, homeobox B8.

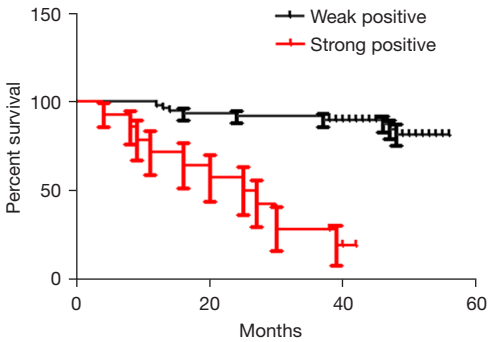

Figure 2 Effect of *HOXB8* on the survival time of patients with NSCLC. HOXB8, homeobox B8; NSCLC, non-small cell lung cancer.

HOXB8 promoted epithelial-mesenchymal transition (EMT)

To investigate the mechanism by which *HOXB8* regulates the biological behavior of lung cancer cells, we assessed the expression of key molecules involved in EMT, including E-cadherin, N-cadherin, vimentin, MMP2, and twist. The results showed that EMT was inhibited by the downregulation of *HOXB8* expression, as E-cadherin expression was upregulated while that of the other proteins was downregulated (*Figure 4*).

Discussion

In this study, we found that *HOXB8* was significantly

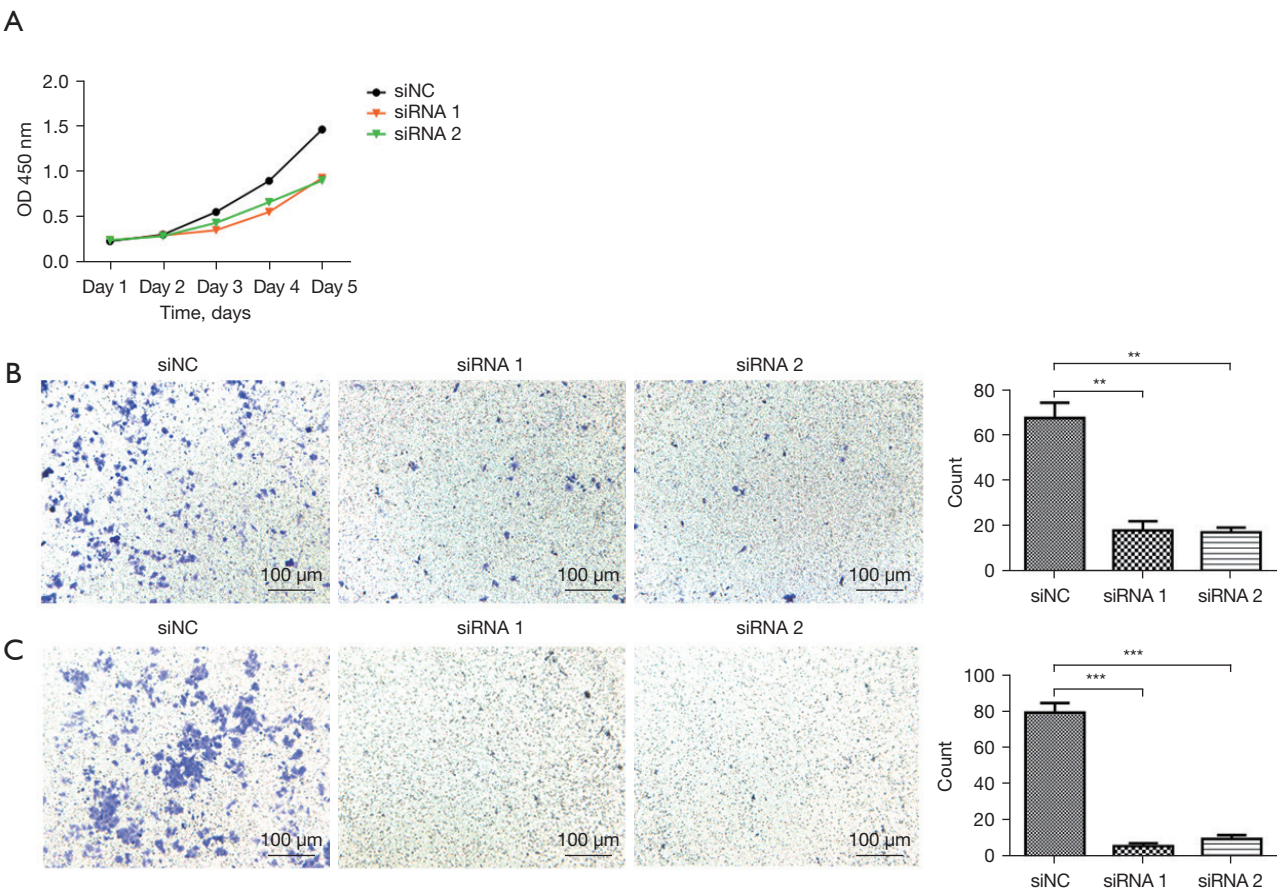

Figure 3 The effect of HOXB8 on the biological behavior of lung cancer cell line A549. (A) CCK-8 experiment. (B) Transwell experiment (stained with hexamethylpararosaniline). (C) Matrigel experiment (crystal violet staining). ** P<0.01, low cell proliferation rate; ***, P<0.001, high cell proliferation rate. OD, optical density; siNC, small interfering RNA negative control; siRNA, small interfering RNA; HOXB8, homeobox B8; CCK-8, Cell Counting Kit 8.

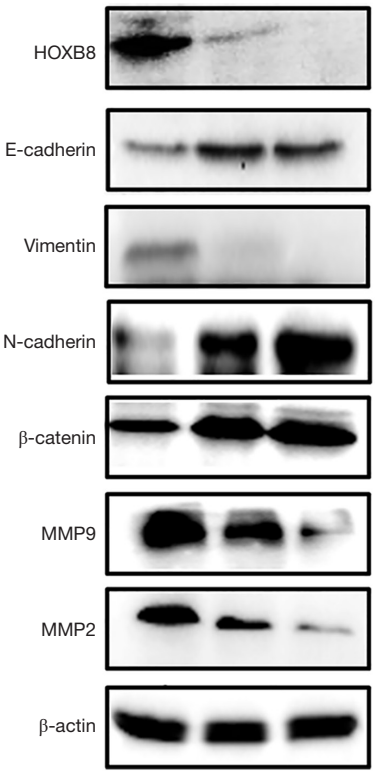

Figure 4 The effect of HOXB8 on EMT-related proteins. HOXB8, homeobox B8; MMP9, matrix metalloproteinase 9; MMP2, matrix metalloproteinase 2; EMT, epithelial-mesenchymal transition.

upregulated in NSCLC tissue compared with adjacent normal tissues. After knockdown of *HOXB8* expression with siRNAs, the proliferation, migration, and invasion abilities of A549 lung cancer cells (A549 cells were isolated from the lung tissue of a White, 58-year-old male with lung cancer. This cell line can be used in cancer, immuno-oncology, and toxicology research) were attenuated. We also analyzed the expression of key EMT-related proteins after *HOXB8* knockdown and found that *HOXB8* appeared to influence EMT progression.

HOXB8 expression has been detected in a variety of tumors, including colorectal cancer (11-13), breast cancer (14), oral squamous cell carcinoma (15), pancreatic cancer (16), cholangiocarcinoma (17), gastric cancer (18), and osteosarcoma (19), among others. In most of these reports, *HOXB8* expression was prognostic and higher level of expression predicted poor outcomes. In this study, we examined 75 patients with NSCLC and confirmed that *HOXB8* expression was significantly higher in NSCLC than adjacent normal tissues, as has been reported. Furthermore, we also analyzed the relationships between *HOXB8* expression levels and clinical parameters and found that *HOXB8* levels were correlating with the poor prognostic clinical parameters. Higher expression of *HOXB8* being associated with a shorter survival period. These results confirm the findings reported in other study (20).

The biological characteristics of tumor cells include rapid proliferation, invasion, and migration. In this study, we explored the biological function of the lung cancer cell line A549 on the knockdown of *HOXB8*. The results showed that the proliferation, migration, and invasion of A549 lung cancer cells were decreased after *HOXB8* expression knockdown, indicating that *HOXB8* can promote lung cancer cell progression. Similar findings have also been reported by other scholars (17,18). Li *et al.* (12) demonstrated that knockdown of *HOXB8* expression in the colorectal cancer cell line, HCT116, decreased its proliferation. Moreover, the invasiveness of HCT116 cells was significantly reduced, and *HOXB8* knockdown promoted HCT116 cell apoptosis. Wang *et al.* reported that *HOXB8* knockdown inhibited colorectal cancer cell proliferation and invasion *in vitro* as well as carcinogenesis and metastasis *in vivo* (13). Yan *et al.* reported that high expression of *HOXB3* predicts poor prognosis and correlates with tumor immunity in lung adenocarcinoma (20).

EMT is a process vital for cancer cell migration and invasion, in which epithelial cells gradually lose their epithelial differentiation characteristics and obtain a mesenchymal phenotype. During EMT, the adhesion between epithelial cells and epithelial cell polarity are gradually lost, with increased changes in cell cytoskeleton and morphology (including increased development of cell pseudopodia) as well as increased cell motility, leading to upregulation of cell migration and invasion ability. In the process of embryonic development and organ formation, cells can spread and migrate between tissues via EMT, after which they continue to grow and differentiate. In addition, EMT can be activated during wound healing, tissue fibrosis, and tumor metastasis. The molecular mechanisms involved in EMT in epithelial cells are complex, and the signaling pathways involved play regulatory roles at the transcription, translation, and post-translation levels. EMT mainly involves regulation of calcium-dependent cell adhesion molecules that maintain epithelial cell properties. For example, cadherin switching, the transition from E-cadherin to N-cadherin, is characterized by loss of E-cadherin function and enhancement of N-cadherin and vimentin.

E-cadherin is a transmembrane glycoprotein encoded by the cadherin-1 gene (*CDH1*) (21); it is a member of the cadherin superfamily and, as a Ca^{2+} dependent adhesion molecule, can regulate intercellular interactions (22). Furthermore, E-cadherin is a calcium-dependent cell-surface protein that promotes epithelial cell adhesion and has long peptide cytoplasmic and extracellular domains. The extracellular domain produces affinity between adjacent cells to promote cell adhesion. E-cadherin is a typical epithelial cell marker of EMT, and inhibiting or blocking E-cadherin expression or function can result in morphological changes of the intercellular matrix conducive to cell migration, invasion, and metastasis (23). Somatic mutation, chromosome deletion, and proteolytic enzyme cleavage can silence or reduce *CDH1* expression levels. In addition, silencing of the *CDH1* promoter by epigenetic modification can also reduce E-cadherin expression, thus promoting a fibroblast phenotype in epithelial cells and enhancing their dissociation and migration abilities. In addition, the transcription factors twist, snail, slug, ZEB1 (zinc finger E-box binding protein 1), and ZEB2 (zinc finger E-box binding protein 2) are transcriptional repressors of E-cadherin and can destroy tight junctions and desmosomes by inhibiting E-cadherin expression. Cadherin switching (the transition from E-cadherin to N-cadherin) regulates cell migration and invasion during EMT. N-cadherin regulates EMT marker proteins, such as E-cadherin and vimentin, by activating mitogen-activated protein kinase (MAPK)/extracellular signal regulated kinase (ERK) and the phosphatidylinositol 3-kinase (PI3K)/protein kinase B (PKB) signal transduction pathways to promote EMT and tumor metastasis. Downregulation of N-cadherin expression has been shown to significantly inhibit the expression of twist, snail, and slug. MMPs can degrade extracellular matrix and reduce cell matrix adhesion (24), and they have important regulatory roles in EMT. The overexpression of MMPs is key to tumor cell migration and invasion, and their mechanism of action follows the same basic pattern of their promotion of EMT during embryonic development, including destruction of cell adhesion, loss of polarity, cytoskeleton remodeling, and the release of stromal-specific MMPs (25).

Conclusions

We found that *HOXB8* levels were increased in lung cancer tissues and cells and that its levels were associated with advanced disease stage and metastasis. EMT was inhibited by the downregulation of *HOXB8* expression, as E-cadherin expression was upregulated while that of the other proteins was downregulated. Thus, *HOXB8* promotes the proliferation, migration, and invasion of lung cancer cells.

Acknowledgments

Funding: None.

Footnote

Reporting Checklist: The authors have completed the REMARK reporting checklist. Available at https://tcr.amegroups.com/article/view/10.21037/tcr-23-2344/rc

Data Sharing Statement: Available at https://tcr.amegroups.com/article/view/10.21037/tcr-23-2344/dss

Peer Review File: Available at https://tcr.amegroups.com/article/view/10.21037/tcr-23-2344/prf

Conflicts of Interest: All authors have completed the ICMJE uniform disclosure form (available at https://tcr.amegroups.com/article/view/10.21037/tcr-23-2344/coif). The authors have no conflicts of interest to declare.

Ethical Statement: The authors are accountable for all aspects of the work in ensuring that questions related to the accuracy or integrity of any part of the work are appropriately investigated and resolved.

References

1. Zheng R, Zeng H, Zhang S, et al. National estimates of cancer prevalence in China, 2011. Cancer Lett 2016;370:33-8.
2. Travis WD, Brambilla E, Nicholson AG, et al. The 2015 World Health Organization Classification of Lung

Tumors: Impact of Genetic, Clinical and Radiologic Advances Since the 2004 Classification. J Thorac Oncol 2015;10:1243-60.
3. Bhatia SJ. Indian Journal of Gastroenterology-May-June 2023 - highlights. Indian J Gastroenterol 2023;42:299-303.
4. Gupta S, Hashimoto RF. Dynamical Analysis of a Boolean Network Model of the Oncogene Role of lncRNA ANRIL and lncRNA UFC1 in Non-Small Cell Lung Cancer. Biomolecules 2022;12:420.
5. Holland PW. Evolution of homeobox genes. Wiley Interdiscip Rev Dev Biol 2013;2:31-45.
6. Ghosh P, Sagerström CG. Developing roles for Hox proteins in hindbrain gene regulatory networks. Int J Dev Biol 2018;62:767-74.
7. Zhu B, Zheng Y, Pham AD, et al. Monoubiquitination of human histone H2B: the factors involved and their roles in HOX gene regulation. Mol Cell 2005;20:601-11.
8. Miller DF, Holtzman SL, Kalkbrenner A, et al. Homeotic Complex (Hox) gene regulation and homeosis in the mesoderm of the Drosophila melanogaster embryo: the roles of signal transduction and cell autonomous regulation. Mech Dev 2001;102:17-32.
9. Vogels R, de Graaff W, Deschamps J. Expression of the murine homeobox-containing gene Hox-2.3 suggests multiple time-dependent and tissue-specific roles during development. Development 1990;110:1159-68.
10. Xie J, Yuan Y, Liu Z, et al. CMTM3 is frequently reduced in clear cell renal cell carcinoma and exhibits tumor suppressor activities. Clin Transl Oncol 2014;16:402-9.
11. Ying Y, Wang Y, Huang X, et al. Oncogenic HOXB8 is driven by MYC-regulated super-enhancer and potentiates colorectal cancer invasiveness via BACH1. Oncogene 2020;39:1004-17.
12. Li X, Lin H, Jiang F, et al. Knock-Down of HOXB8 Prohibits Proliferation and Migration of Colorectal Cancer Cells via Wnt/β-Catenin Signaling Pathway. Med Sci Monit 2019;25:711-20.
13. Wang T, Lin F, Sun X, et al. HOXB8 enhances the proliferation and metastasis of colorectal cancer cells by promoting EMT via STAT3 activation. Cancer Cell Int 2019;19:3.
14. Garcia SAB, Araújo M, Freitas R. Dataset of HOXB7, HOXB8 and HOXB9 expression profiles in cell lines representative of the breast cancer molecular subtypes Luminal a (MCF7), Luminal b (BT474), HER2+ (SKBR3) and triple-negative (MDA231, MDA468), compared to a model of normal cells (MCF10A). Data Brief 2020;30:105572.
15. Lu N, Yin Y, Yao Y, et al. SNHG3/miR-2682-5p/HOXB8 promotes cell proliferation and migration in oral squamous cell carcinoma. Oral Dis 2021;27:1161-70.
16. Zhang L, Wang Y, Zhang L, et al. LINC01006 promotes cell proliferation and metastasis in pancreatic cancer via miR-2682-5p/HOXB8 axis. Cancer Cell Int 2019;19:320.
17. Jiang X, Li J, Wang W, et al. AR-induced ZEB1-AS1 represents poor prognosis in cholangiocarcinoma and facilitates tumor stemness, proliferation and invasion through mediating miR-133b/HOXB8. Aging (Albany NY) 2020;12:1237-55.
18. Ding WJ, Zhou M, Chen MM, et al. HOXB8 promotes tumor metastasis and the epithelial-mesenchymal transition via ZEB2 targets in gastric cancer. J Cancer Res Clin Oncol 2017;143:385-97.
19. Guo J, Zhang T, Dou D. Knockdown of HOXB8 inhibits tumor growth and metastasis by the inactivation of Wnt/β-catenin signaling pathway in osteosarcoma. Eur J Pharmacol 2019;854:22-7.
20. Yan M, Yin X, Zhang L, et al. High expression of HOXB3 predicts poor prognosis and correlates with tumor immunity in lung adenocarcinoma. Mol Biol Rep 2022;49:2607-18.
21. Felipe Lima J, Nofech-Mozes S, Bayani J, et al. EMT in Breast Carcinoma-A Review. J Clin Med 2016;5:65.
22. Yang Q, Cao X, Tao G, et al. Effects of FOXJ2 on TGF-β1-induced epithelial-mesenchymal transition through Notch signaling pathway in non-small lung cancer. Cell Biol Int 2017;41:79-83.
23. Liu F, Gu LN, Shan BE, et al. Biomarkers for EMT and MET in breast cancer: An update. Oncol Lett 2016;12:4869-76.
24. Kaufhold S, Bonavida B. Central role of Snail1 in the regulation of EMT and resistance in cancer: a target for therapeutic intervention. J Exp Clin Cancer Res 2014;33:62.
25. Zhou XM, Zhang H, Han X. Role of epithelial to mesenchymal transition proteins in gynecological cancers: pathological and therapeutic perspectives. Tumour Biol 2014;35:9523-30.

Cite this article as: Jiang S, Wang T, Han Y, Hida T, Afzal MZ, Zhou C, Zhu J, Wang H. Downregulation of homeobox B8 in attenuating non-small cell lung cancer cell migration and invasion though the epithelial-mesenchymal transition pathway. Transl Cancer Res 2024;13(1):413-422. doi: 10.21037/tcr-23-2344

